Indian Journal of Chemistry
Vol. 58A, March 2019, pp. 330-334

Sonochemical synthesis of palladium nanoparticles and its electrocatalytic activity for oxidation of formic acid

Hong Du*, Xiaohui Sun & Shuxian Zhao

College of Chemistry and Chemical Engineering, Xinjiang Normal University, Urumqi 830054, China
Email: 175790509@qq.com

Received 6 September 2018; revised and accepted 8 February 2019

Monodispersed palladium nanoparticles have been synthesized from palladium(II) chloride aqueous solution by ultrasonication without gas protection and in the absence of an external reducing agent, by the addition of a small quantity of polyvinylpyrrolidone (PVP). The monodispersity and columnar crystallinity of palladium nanoparticles have been observed using TEM and HRTEM respectively. The five X-ray diffraction peaks of the metallic Pd indicated that Pd(II) ions have been reduced to palladium atoms Pd(0). The formation of nanoparticles has been investigated using FT-IR spectroscopy. Results show that the PVP can protect metal nanoparticles via the coordination of the PVP carbonyl group to the palladium atoms and the steric effect of the PVP polymer long chain. The activity towards formic acid oxidation reaction (FAOR) has also been measured.

Keywords: Palladium, Nanoparticles, Polyvinypyrrolidone, Palldium(II) chloride, Ultrasonic

Nanophase materials find many applications in chemistry, optics, electricity, magnetism, etc[1]. Being used as efficient hydrogen storage materials, sensors, in biomedicine and as heterogeneous catalytic materials, nano-palladium has attracted worldwide attention[2-5]. Particularly, much effort has been directed towards the preparation of palladium nanoparticles. Nowadays, nano-palladium nanoparticles of different shapes and sizes can be prepared by a variety of techniques such as chemical reduction of $PdCl_2$ in the presence of $NaBH_4$ and other reducing agents[6], via hydrothermal reaction[7], ultrasonic restoration of $PdCl_2$ in systems containing reducing agent[8], etc. Among these techniques, ultrasonication based on its special mode of action has been developed into a new technology for preparing nano-palladium particles.

In various palladium salt solutions, nano-palladium particles, fabricated by ultrasonic technology under an inert atmosphere, in the presence of a reducing agent, present smaller grain size and narrower size distribution than that of those prepared by other techniques. However, the presence of an inert atmosphere shielding makes the reaction system complicated. While reducing agents such as nutmeg-based trimethylamine, ethylene glycol or ascorbic acid, etc.,[9-12] participate in chemical reaction and often speed up the rate of ion reduction, which leads to the formation of large seed crystals. So the dispersion of crystal grains becomes difficult, palladium nanoparticles aggregate and the size increases accordingly. Herein, we report the preparation of monodisperse palladium nanoparticles by *in situ* ultrasonication without any atmospheric shielding or additional/external reducing agent, but employing PVP as the dispersion stabilizer, water as the medium and palladium chloride as the precursor of reaction. The microstructure of nanoparticles and the dispersion mechanism were investigated as well.

Experimental

The Pd nanoparticles were synthesized by ultrasonication without gas protection and reductant using aqueous solutions of palladium chloride ($PdCl_2$). In a typical synthesis, 30 mg of $PdCl_2$ was dissolved in 60 mL double distilled water. Then the mixture was sonicated in the ultrasonic device (Model TY98-III with an ultrasound power of 200 W and frequencies of 20 kHz) to react for 6 min at a temperature of 318±2 K. The obtained black suspension was marked as Sample A. For the synthesis of monodispersed palladium nanoparticles, 30 mg of $PdCl_2$ and 300 mg of PVP were added into 60 mL double distilled water and the above procedure was repeated. The obtained sample was labelled as Sample B.

Synthesis of reduced graphene oxide (rGO) was carried out as follows. The GO was functionalized in acidic medium for 5 h, stirring at an elevated temperature (30 °C). The functionalized GO was dispersed in double distilled water and sonicated for 3 h. Then the suspension was transferred into an autoclave and hydrothermally treated at 483 K for 24 h to obtain rGO.

For the anchoring of Pd nanoparticles on rGO, 1 mg/mL solution containing rGO was dispersed in double distilled water. Pd nanoparticles (1 mg/mL) solution was added into the above suspension. This suspension mixture was stirred at 303 K for 5 h.

The electrochemical activity of Pd nanoparticles was also evaluated. Prior to each electrochemical measurement, a glassy carbon (GC) working electrode (0.196 cm^2 geometric surface area) was first polished. The alumina slurries (Al_2O_3, 0.05 mm) were applied on a polishing substrate to obtain a mirror finishing, To develop a catalyst coated GCE, 15 mL of the 1 mg/mL sample (Pd nanoparticles Pd/rGO composite) suspension in double distilled water was pipetted on the polished electrode surface by a micro-liter syringe, after drying in vacuum at room temperature. Then the catalyst was coated with a thin Nafion (0.1 wt% in water, 5 mL) layer to ensure that the catalyst was fixed to the GCE surface during the electrochemical experiments. Cyclic voltammetry measurements were performed with a CHI660D electrochemical work-station. The electrode prepared in the above steps was used as the working electrode. The Ag/AgCl electrode was used as the reference electrode and isolated in a double-junction chamber and a Pt coil was used as the counter electrode. All the electrochemical experiments were done with respect to the standard values of the reversible hydrogen electrode (RHE). N_2 gas (Infra, 99.999%) was used to maintain an inert atmosphere. Cyclic voltammetry was performed in 0.1 M $HClO_4$ solution as basic media.

Results and discussion

The variation in the color of reaction system of sample B is shown in supplementary data, Fig. S1. It can be seen that the color changed from pale yellow to dark brown, which is the same as the color of reaction systems of Sample A. This observation indicates the reduction of Pd(II) ions to palladium atoms Pd(0). Notably, it can be observed that the color of reaction system of Sample B seems to change faster than that of Sample A.

It has been reported[13] that the sonochemical process may occur in three different regions viz., (1) inside the collapsed bubbles where extremely high temperature and pressure are provided; here the water vapor is further transformed into •H and •OH; (2) the interfacial region between the cavitation bubbles and the bulk solution, where temperature is lower than that within the cavitation bubbles, but high enough to induce sonochemical transformation; (3) the bulk solution segment under the ambient temperature, which is the reaction area for reactant molecules with •H or •OH.

The chemical effects of ultrasonication originate from its acoustic cavitation: formation, oscillation, growth, and implosive collapse of bubbles in the liquid. The collapsing of cavitations of bubbles produces instantaneous, localized high temperature (~5000 K) and high pressure (~20 MPa) within a highly confined space around the cavitation bubbles over a minimum interval. Accompanied by strong shock wave and/or jet current whose speed is 400 kmph, the concentrated high energy can initiate the synthesis of a new phase.

In preparing the reaction system of Sample A, H_2O would absorb ultrasonic energy to produce •H and •OH. Due to the high oxidizing potential of Pd^{2+} (+0.92 V), •H could reduce Pd^{2+} to Pd(0) atom. It has been reported that the surfactants in water are subjected to pyrolysis by ultrasonic irradiation to give some radicals such as $•CH_3$, etc. Such radicals would be formed in preparing the reaction system of Sample B, and these radicals contribute to the increase in the rate of reduction of Pd(II):

$RH \rightarrow$ reducing radicals + $•CH_3$ etc.

$•CH_3$ etc. + $RH \rightarrow CH_4$ etc. + reducing radicals

Pd(II) + reducing radicals $\rightarrow\rightarrow$Pd(0)

In addition, owing to the rapid reaction, it is difficult to control the deoxidization rate, which leads to the agglomeration of Pd(0) nanoparticles, deepening the color quickly. Only several minutes later when the reaction ended, the suspension began to delaminate with brown granular deposits at the bottom of the beaker. While in preparing the reaction system of Sample B, N and O on PVP molecules and Pd^{2+} form the coordinated complex ion to lower the oxidizing potential of palladium ion. The coordinated complex ion reacts with •H, which effectively controls the deoxidization speed of palladium ion. Palladium crystal cluster is obtained from the deoxidization, and, the surface of metal particles is covered and absorbed by the long chain of PVP. Hence Pd particles suspend well within the solution and the agglomeration among Pd particles is avoided. The possible mechanism is depicted in Scheme 1.

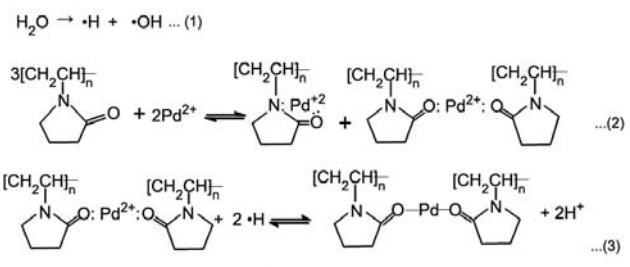

Scheme 1

Consequently, it is concluded that PVP acts as the reductive agent for the reduction of Pd(II) in the sonochemical process , in addition to serving as the stabilizer of palladium particles

The pH values of the samples of palladium solution decrease from 4.50 before the reaction to 2.50 after the reaction. This variation is presumably ascribed to the amount of produced Pd(0) atoms which increases the H^+ ion concentration in the ultrasonicated solutions, according to step 3 of Scheme 1. At the end of the reaction, the nano-palladium suspension liquid gradually turns black due to its absorbing of visible light. The stability of dispersion is so good that no delaminating appears even 5 months later, which is consistent with the result of the nano-palladium system prepared by Ca´rdenas-Trivino[14].

In the reaction system of Sample A, the shape of the prepared nano-palladium particles is irregular and its grain size is around 20 nm with a wider distribution range because of the absence of PVP. Moreover, the nano-palladium particles agglomerate to form nano-palladium clusters with different sizes (Fig. 1a). While in the reaction system of Sample B obtained by adding PVP as the protective agent, the coordination effect between PVP and palladium nanoparticles as well as the effect of space resistance of PVP long chain structure have wrapped up the nano-palladium particles so that the nano-palladium particles are distributed well without any agglomeration[15] (Fig. 1b). The shape of nano-palladium particles is basically spherical with a narrow distribution of about 10 nm. The agglomeration of nano-palladium particles has been efficiently prevented. Comparing with nano-palladium particles prepared in the reaction system with reducing agent under the same ultrasonic condition[9,16], the distribution of sample B is even better with smaller size. The result is similar to the nano-palladium system prepared by Pandian Kannaiyan[17]. The nano-palladium particles as shown in Fig. 1b are columnar crystals. The observation of lattice fringes (Fig. 1c) indicates that the formed nano-palladium particles have good crystallinity. The interplanar spacings of d_{111} derived from the lattice fringes are 0.226 nm for both Pd(0), which are coincide well with the theoretical values (d_{111} = 0.227 nm). On the surface and corner of (111), there are some atomic high surface steps which possibly have significance in improving the catalysis of nano-palladium particles.

X-Ray diffraction (XRD) pattern of Sample B is displayed in Fig 2. The diffraction peaks of simple PVP/Pd nano-composite sample display five prominent diffraction peaks at 39.74°, 46.37°, 67.7°, 81.68° and 86.2°corresponding to (111), (200), (220), (311) and (222) planes, respectively, which match well with the standard value peaks (JCPDF card No. 5-681). The wide peak at around 20° is the diffraction maximum resulting from by PVP polymer[18].

The FT-IR spectra of PVP and nano-Pd with PVP samples are shown in supplementary data, Fig. S2a. In all spectra, there are absorption peaks from 500 cm^{-1} to 3500 cm^{-1}. The absorption bands appearing in the 1600~1680 cm^{-1} range are assigned to the stretching vibration mode of the PVP carbonyl in the nanoparticles. The bands at 1290 cm^{-1} and 2954 cm^{-1} are attributed to the C-N stretching vibration and alkyl characteristic peak respectively. The wide absorption

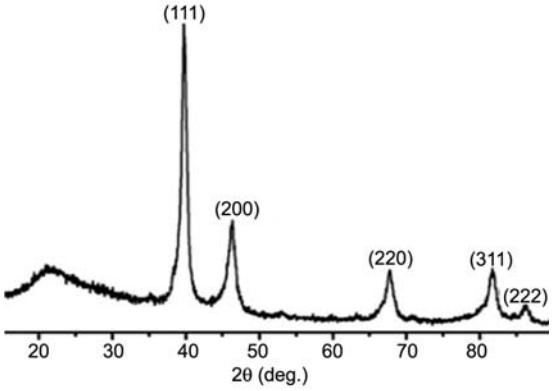

Fig. 2 — XRD pattern of nano-Pd with PVP sample.

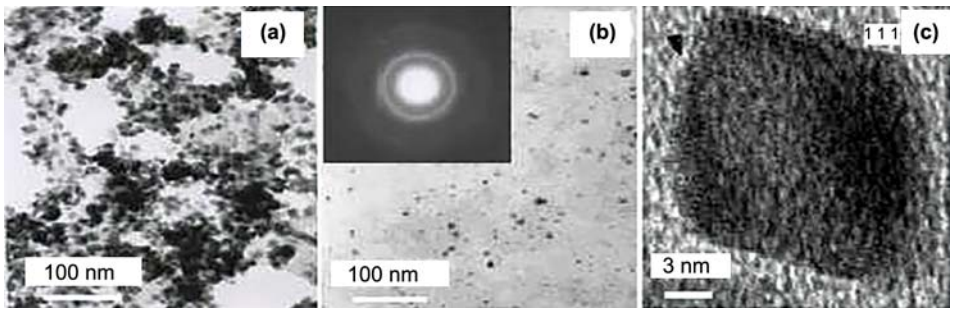

Fig. 1 — HRTEM images of (a) nano-Pd without PVP (b) nano-Pd with PVP and (c) SAED pattern.

band within 3000~3500 cm^{-1} might come from the absorption peak of PVP absorbed water, the partially enlarged spectra is provided as Fig. S2b. Compared with pure PVP, the PVP carbonyl absorption peak in the nano-palladium composite powder, moves towards the low frequency direction, changing from 1664 cm^{-1} to 1656 cm^{-1}, which is essentially due to interaction of the C=O (PVP) with the palladium nanoparticle surface. According to the analysis of research of Yang *et al*.[19] and Pan *et al*., [20] the reason for the stabilization of the formed palladium nanoparticles is likely due to the following two aspects: (i) the adsorption of the PVP chain on the palladium particle surface stabilizes and disperses nano-palladium particles due to the hydrophilicity of PVP side chain; (ii) the PVP polymer long chain and its hydrophobicity increase the steric hindrance which can protect the palladium nanoparticles.

The electrochemical activity of Pd nanoparticles, was tested in N_2 saturated 0.1 M $HClO_4$ solution. The base CVs showed in Fig. 3 present the typical hydrogen adsorption-desorption and surface oxidation-reduction reaction of Pd nanoparticles. In all the CVs, the hydrogen adsorption-desorption area (0 to 0.3 V) is ascribable to the hydrogen desorption from Pd (100) planes. The more Pd nanoparticles are enriched with Pd (100) planes, the more the effect. The oxidation peak potential of 0.80 V, the reduction peak potential of 0.75 V and electrochemical characteristics testify to the well-defined Pd nanoparticles in all the catalysts[21]. The effective improvement in the size of electrical double layer (EDL) area in Pd/rGO by contrast with the Pd nanoparticles arises from rGO support material[22,23]. The EDL area explicates the interplay of the solid catalyst surface with the solution. The EDL area broadens in our research for Pd/rGO in line with previous reports[24]. Typical base CV for Pd supported nanoparticles on carbon powders composite exhibit higher surface to volume ratio value with higher active area for electrochemical procedure.

The formic acid oxidation reaction (FAOR) activity of Pd and Pd/rGO catalysts is also measured with Pd/rGO catalyst, as showed in Fig. 4. The Pd nanoparticles exhibited very low FAOR activity, but the reduction and oxidation peaks began to appear. As the rGO was introduced, the FAOR activity was obviously enhanced. The peak current in the positive scan was larger than that of in the in the negative scan during HCOOH electrooxidation by Pd/rGO, which indicated that

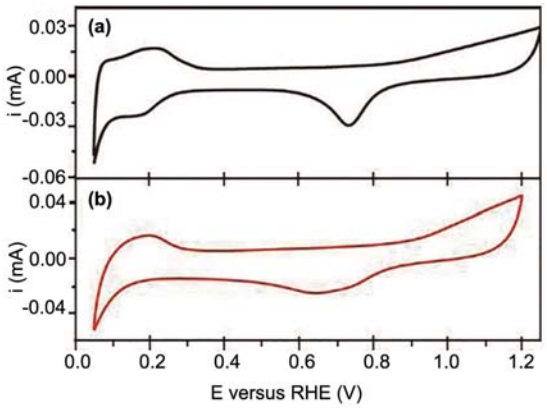

Fig. 3 — Base CVs for (a) unsupported Pd nanoparticles and (b) supported nanoparticles on carbon powders composite in 0.1 M $HClO_4$ solution at 50 mV/s.

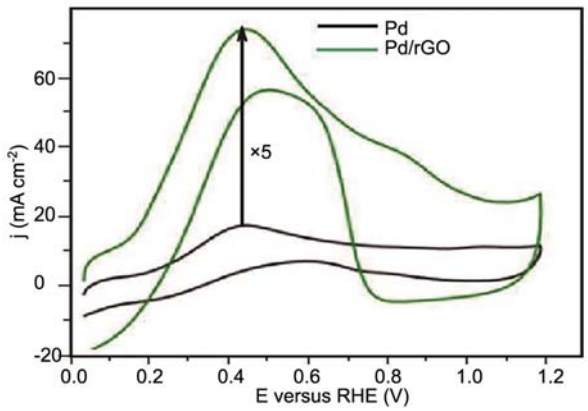

Fig. 4 — CV results of formic acid oxidation reaction for all catalysts in 0.1 M $HClO_4$ + 1 M HCOOH solution at 50 mV/s.

Pd/rGO catalyst shows superior tolerance to CO poisoning, and that the formic acid oxidation reaction follows direct oxidation mechanism. Pd catalyst may be obedient to a direct dehydrogenation pathway during FAOR[25,26]. It is noted that the FAOR activity of Pd/rGO catalyst is five-fold higher than the Pd catalyst. This higher activity may be attributed to the synergistic effect of rGO in the catalyst.

In summary, it has been demonstrated that the synthesis of palladium nanoparticles with mean sizes of about 10 nm can be successfully carried out by sonochemical reduction of palladium(II) chloride in aqueous solution, in the presence of PVP as a stabilizing agent without any other reductant. Complexation effect between PVP and palladium nanoparticles could effectively control the reduction rate of nano-palladium particles and hence the highly dispersed and even-shaped nano-palladium particles could be prepared by *in situ* ultrasonication to

overcome the agglomeration. Furthermore, the bulk shielding capacity formed by the absorption and hydrophilic performance of PVP contributed to the high dispersion stability of nano-palladium particles. The products obtained in the presence of PVP are columnar nanostructures, with a narrow distribution of about 10 nm. Palladium nanoparticles are loaded over rGO composite support. The activity towards formic acid oxidation reaction is investigated and compared with Pd nanoparticles. The improvement in the activity of Pd nanoparticles has been observed after anchoring on rGO. The improvement in electrocatalytic activity is considered as a result of synergistic effect induced by rGO.

Supplementary data

Supplementary data associated with this article are available in the electronic form at http://www.niscair.res.in/jinfo/ijca/IJCA_58A(03)330-334_SupplData.pdf.

Acknowledgement

This study was supported by the National Natural Science Foundation of Xinjiang (2017D01A56).

References

1 Alam M N, Roy N, Mandal D & Begum N A, *RSC Adv*, 3 (2013) 11935.
2 Yuan M, Liu A, Zhao M, Dong W J, Zhao T Y, Wang J J & Tang W H, *Sens Actuators B*, 190 (2014) 707.
3 Cheng N N, Wang H J, Li X M, Yang X Y & Zhu L D, *Am J Anal Chem*, 3 (2012) 312.
4 Gobal F & Faraji M, *J Electroanal Chem*, 691 (2013) 51.
5 Zhang J, Xu Y & Zhang B, *Chem Comm*, 50 (2014) 13451.
6 Hu J, Zhou Z, Zhang R, Li L & Cheng Z, *J Mol Catal A Chem*, 381 (2014) 61.
7 Fu G, Tao L, Zhang M, Chen Y, Tang Y, Lin J & Lu T, *Nanoscale*, 5 (2013) 8007.
8 Ghanbari N, Hoseini S J & Bahrami M, *Ultrason Sonochem*, 39 (2017) 467.
9 Zhao Y, Jia L & Medrano J A, Ross J R H & Lefferts L, *ACS Catal*, 3 (2013) 2341.
10 Borkowski T, Zawartka W, Pospiech P, Mizerska U, Trzeciak A M, Cypryk M & Tylus W, *J Catal*, 282 (2011) 270.
11 Su C, Zhao S, Wang P, Chang W W, Chang K S & Zhang H B, *J Environ Chem Eng*, 4 (2016) 3433.
12 Gopalakrishnan R, Loganathan B, Dinesh S & Raghu K, *J Cluster Sci*, 28 (2017) 1.
13 Yao K, Dong Y Y, Bian J, Ma M G & Li J F, *Ultrason Sonochem*, 24 (2015) 27.
14 Cárdenas-Triviño G, Segura R A & Reyes-Gasga J, *Coll Polym Sci*, 282 (2004) 1206.
15 Xu Y, Chen L, Wang X, Yao W & Zhang Q, *Nanoscale*, 7 (2015) 10559.
16 Kettemann F, Wuithschick M, Caputo G, Kraehnert R, Pinna N, Rademann K & Polte J, *Eur J Endocrinol*, 17 (*2015*) 238.
17 Kannaiyan P, *Int J ChemTech Res*, 7 (2015) 1297.
18 Saldan I, Semenyuk Y, Marchuk I & Reshetnyak O, *J Mater Sci*, 50 (2015) 2337.
19 Yang Z S & Wu J J, *Fuel Cells*, 12 (2012) 420.
20 An H, Pan L N, Cui H, Wang B, Zhai J P, Lin Q & Pan Y, *Electroanal*, 27 (2015) 1925.
21 Erikson H, Sarapuu A, Alexeyeva N, Tammeveski K, Solla-Gullon J & Feliu J M, *Electrochim Acta,* 59 (2012) 329.
22 Hara M, Linke U & Wandlowski T, *Electrochim Acta,* 52 (2007) 5733.
23 Hoshi N, Kagaya K & Hori Y, *J Electroanal Chem,* 485 (2000), 55.
24 Henstridge M C, Dickinson E J F & Compton R G, *Chem Phys Lett*, 485 (2010) 167.
25 Neurock M, Janik M & Wieckowski A, *Faraday Discuss*, 140 (2008) 363.
26 Chen Y X, Heinen M, Jusys Z & Behm R J, *Angew Chem Int Ed*, 45 (2006) 981.